Macro-motion Detection Using Ultra-wideband Impulse Radar

Xin Li, Dengyu Qiao, and Ye Li*, *IEEE Member*

***Abstract*— Radar has the advantage of being able to detect hidden individuals, which can be used in homeland security, disaster rescue, and healthcare monitoring-related applications. Human macro-motion detection using ultra-wideband impulse radar is studied in this paper. First, a frequency domain analysis is carried out to show that the macro-motion yields a bandpass signal in slow-time. Second, the FTFW (fast-time frequency windowing), which has the advantage of avoiding the measuring range reduction, and the HLF (high-pass linear-phase filter), which can preserve the motion signal effectively, are proposed to preprocess the radar echo. Last, a threshold decision method, based on the energy detector structure, is presented.**

I. Introduction

In homeland security, disaster rescue, and healthcare monitoring-related applications, radar has the advantage of being able to detect, locate and monitor individuals, even if the human bodies are obscured by obstacles. Using ultra-wideband (UWB) impulse radar to detect human motion [1-3] has been studied recent years, e.g., searching survivors in debris after disaster by detecting the breathing motion of human body [4-8].

Human motion generally can be divided into two types, micro-motion and macro-motion [9]. The former indicates the human motion in the same range cell, such as standing with arm swinging, and breathing. The latter indicates the motion that human target moves from one range cell to another, like walking and running. In this paper, the detection of macro-motion using UWB impulse radar is studied.

The detection commonly includes two steps. The first is the preprocessing of the raw echo samples. The raw echo samples are made up of several signal components, i.e., the target signal and the interference signals. The former is the echo of the moving body. The latter mainly contain the stationary clutter (the echo of the static background), the noise, the linear-trend [10], the wireless interference caused by the communication systems, and the fast-time DC component introduced by the sampling system. By signal preprocessing algorithms, such as the digital filter [4-6], the mean subtraction (MS) algorithm [2], the linear trend subtraction (LTS) algorithm [4-6, 10], and the background subtraction (BS) algorithms [9, 11, 12], the interference signals will be suppressed.

The second step of the detection is the threshold decision. For breathing motion detection, several threshold-decision methods have been offered. In [4], singular value decomposition (SVD) in frequency domain and constant false alarm threshold were used to decide the existence of the respiratory signal. In [5], the respiratory signal of the trapped victim was identified by range-frequency windowing. In [6], a threshold-decision method was proposed based on harmogram. However, there appears to be little relevant work in offering a threshold-decision method for the macro-motion detection. In [9, 12], the macro-motion was identified by manual inspection from the processed experimental data.

This paper is aimed to study the detection of macro-motion using UWB impulse radar, and is organized as follows. In section II, a frequency domain analysis is carried out, which reveals that the macro-motion yields a bandpass signal in slow-time. In section III, the preprocessing techniques are studied, and fast-time frequency windowing (FTFW) and slow-time high-pass linear-phase filter (HLF) are proposed. In section IV, a threshold decision method based on the energy detector [13] is presented. A conclusion is drawn in section V.

II. Frequency Domain Analysis of the Slow-Time Macro-Motion Signal

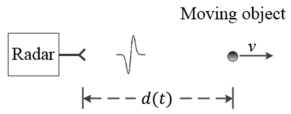

Fig. 1 The sketch: a moving target is measured by radar

For a uniformly moving object with radial velocity v m/s (Fig. 1), the distance from the object to the radar can be written as a function of t [1], that is $d(t) = d_0 + vt$, where d_0 is the initial distance. Let $p(s)$ [1] denote the transmitted radar impulse. The echo of the impulse sent at t can be represented as a fast-time signal as follows,

$$r_t(s) = p\left(s - \frac{2d(t)}{c}\right) = p\left(s - \frac{2v}{c}t - \frac{2d_0}{c}\right), \quad (1)$$

where c denotes light speed. If we regard (1) as a function of t, we can get the expression of the slow-time motion signal as follows,

$$r_s(t) = p(Vt + D), \quad (2)$$

where $V = -2v/c$ and $D = s - 2d_0/c$. Then, the Fourier transform (FT) of $r_s(t)$,

$$R_s(f) = \int_{-\infty}^{+\infty} p(Vt + D)\, e^{-i2\pi ft}\, dt = \frac{e^{-i2\pi fD/V}}{|V|} \int_{-\infty}^{+\infty} p(x)\, e^{-i2\pi \frac{f}{V}x}\, dx. \quad (3)$$

Research is supported in part by the National Science Foundation of China (NO.61379136), Key Lab for Health Informatics of Chinese Academy of Science (NO.CXB201104220026A), and Basic Research Programs of Shenzhen (NO.JC201104220255A and NO.JC201005270258A).

Xin Li (e-mail: stillbluelixin@gmail.com; xin.li@siat.ac.cn), Dengyu Qiao (e-mail: dy.qiao@siat.ac.cn), Ye Li* (e-mail: ye.li@siat.ac.cn), are with the Shenzhen Institutes of Advanced Technology, Chinese Academy of Sciences, Key Lab for Health Informatics of Chinese Academy of Science.

[1] Impulse radar echoes involve two time axis， fast-time and slow-time. In this paper, the time variable in fast-time is denoted by s, and the time variable in slow-time is denoted by t.

Considering that the FT of the radar impulse, $P(f) = \int_{-\infty}^{+\infty} p(s)\, e^{-i2\pi fs}\, ds$, (3) can be rewritten as follows,

$$R_s(f) = \frac{e^{-i2\pi fD/V}}{|V|} P\left(\frac{f}{V}\right). \quad (4)$$

The preceding equation reveals the relation of frequency spectrum between the radar impulse and the slow-time motion signal. If the bandwidth of the radar impulse is $f_L \sim f_U$, then the bandwidth of the slow-time motion signal is $|V|f_L \sim |V|f_U$ [1]. This relation can be demonstrated further by the similarity between the fast-time waveform of the radar impulse (Fig. 2) and the waveform of the slow-time motion signal (Fig. 3 (b)).

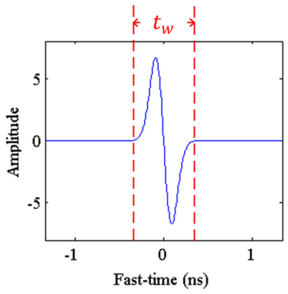

Fig. 2 The radar impulse employed by the experimental radar system

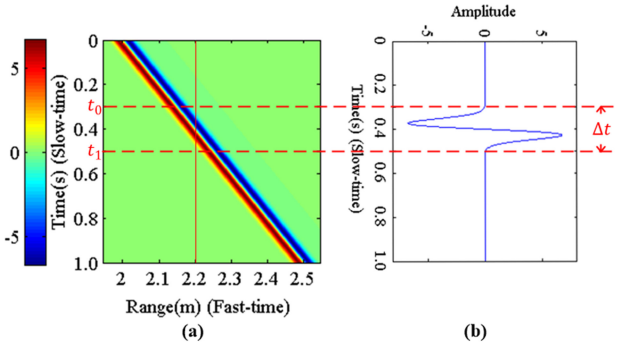

Fig. 3 (a) The echo matrix of the uniformly moving object, which moves from 0.2m to 0.25m with a speed of 0.5m/s. (b) The slow-time motion signal in the range cell of 2.2m.

For a single range cell, the slow-time motion signal is determined by the motion in the short time period when the target echo moves across that range cell. We call this time period the observation time period (OT), and denote its length by Δt. For example, in Fig. 3, the OT of the range cell of 2.2m is the time interval $[t_0, t_1]$, and $\Delta t = t_1 - t_0 \approx 0.2$s.

Parameter Δt depends on the width of the radar impulse, t_w (see Fig. 2), and the speed of the motion, v. It is easy to get

$$\Delta t = \frac{t_w c}{2|v|}. \quad (5)$$

The echo of human body with macro-motion consists of the echoes of individual body parts, mainly including head, torso, upper leg, lower leg, feet, upper arm and lower arm. Although the speeds of these body parts are different and change with time, their motions can be regarded as uniform motions approximately during the very short OT, which means that (4) is still valid.

If the maximal and minimal values of the speeds of all the body parts are v_{max} and v_{min} respectively, then by (4) the bandwidth of the slow-time macro-motion signal will be $|2v_{min}/c|f_L \sim |2v_{max}/c|f_U$. Now, we can conclude that the macro-motion generates a bandpass signal in slow-time [2].

III. Preprocessing of the Raw Echo Samples

The flow chart of the preprocessing of the raw echo samples is presented in Fig. 4, where the raw echo samples are processed firstly in fast-time and then in slow-time.

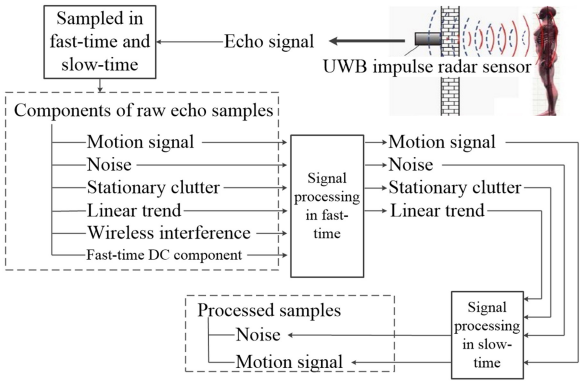

Fig. 4 The flow chart of signal preprocessing

A. Fast-time signal processing

Previous works [4-6] adopted the digital filter as the fast-time signal processing technique. The fast-time DC component and the wireless interference will be suppressed, as these signal components fall into the stop band of the filter. In order to preserve the waveform of the echo, a linear-phase filter should be adopted [6]. But, a drawback of the digital filter is the decrease of the number of the total samples in fast-time, which results in a reduction of the measuring range [3]. Fast-time FFT windowing (FTFW) (Fig. 5) can overcome this drawback. Since a dominant frequency component, due to its leakage in FFT, will make the FW algorithm perform poorly, we use the mean subtraction (MS) algorithm to remove the strong fast-time DC component before the FFT, as shown in Fig. 5.

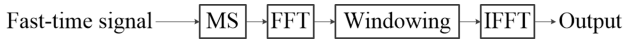

Fig. 5 The flow chart of the FTFW.
FFT: Fast Fourier Transform. **IFFT**: Inverse Fast Fourier Transform.

B. Slow-time signal processing

The slow-time signal processing techniques are used to

[1] For example, suppose that the -10dB bandwidth of the radar impulse is $0.45 \sim 3.6$GHz. If $v = 0.5$m/s, then the -10dB bandwidth of the slow-time motion signal is $1.5 \sim 12$Hz.

[2] In order to simplify the analysis, we do not consider the amplitude attenuation and phase distortion of the radar impulse during the transmission. Although these factors result in changing the frequency spectrum of the radar impulse, no new frequency components will be introduced into the echo. In other word, the energy of echo still distributes within the frequency band of $f_L \sim f_U$, which means that the energy of the slow-time motion signal will still distribute within the frequency band of $|2v_{min}/c|f_L \sim |2v_{max}/c|f_U$. The conclusion that the slow-time macro-motion signal is a band-pass signal is still valid.

[3] Suppose that a FIR filter is adopted, and the filter order is O. If the original number of samples in fast-time is N_{ft}, then after the digital filter, the number of samples reduces to $N_{ft} - O + 1$. As a result, the measuring range becomes $(N_{ft} - O + 1)/N_{ft}$ of the original.

remove the strong stationary clutter, and can be divided into two types, the non-real-time algorithms and the real-time algorithms.

The non-real-time algorithms, e.g., the mean subtraction (MS) algorithm [2], and the linear trend subtraction (LTS) algorithm [4-6, 10], have been employed in the application of micro-motion detection, such as respiration detection. These algorithms cannot operate on a signal in real-time as they have to wait for the whole signal data to be stored before processing them. The non-real-time algorithms are not suitable for the macro-motion detection, which commonly requires a real-time trajectory tracking.

For the real-time algorithms, the two-order moving target indication (TOMTI) [14], the accumulate average background subtraction (AABS) algorithm, the moving average background subtraction (MABS) algorithm, and the exponential average background subtraction (EABS) algorithm [9, 11, 12], have been studied in previous works. The TOMTI is designed based on the estimation of the changes of the echo. The AABS, the MABS, and the EABS, are based on the estimation of the stationary clutter.

These previous real-time algorithms fail to preserve the slow-time motion signal effectively. According to the magnitude response (see Fig. 6 (a)), the motion signal, especially its low-frequency component, will be suppressed by the TOMTI. The non-linear phase response of the MABS (see Fig. 6 (b)) will result in a waveform distortion of the motion signal, e.g., tailing, which also can be seen in the output of the AABS and the EABS (Fig.4 of [9]). In [9], an adaptive tap-length BS algorithm was proposed, which can effectively avoid tailings but requires more computation.

The TOMTI, the MABS and the EABS indeed are slow-time filtering methods, although their derivations are not based on the filter design theory. In this paper, a slow-time high-pass linear-phase filter (HLF) is designed to process the raw echo samples in slow-time. In order to remove the stationary clutter without suppressing the motion signal, the HLF should be a high-pass filter (see Fig. 6 (a)). In order to preserve the waveform of the motion signal, the HLF should be linear-phase (see Fig. 6 (b)).

C. *Experimental results of the signal preprocessing*

Parameter settings of the experimental system are given in Table I. Fig 7 shows the rectangle frequency window of the FTFW, and the impulse response of the FIR (finite impulse response) HLF, which are used in the experiment.

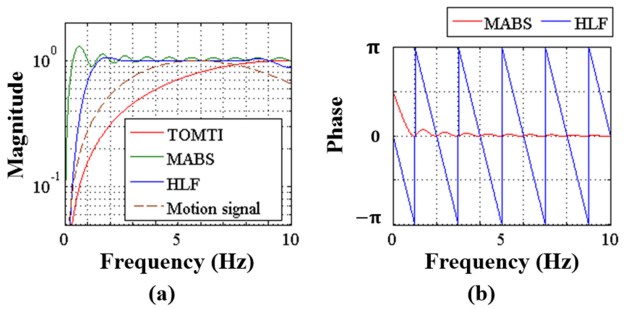

Fig. 6 **(a)** Magnitude responses of the TOMTI, the MABS, and the HLF, and the magnitude spectrum of a slow-time motion signal. **(b)** Phase responses of the MABS and the HLF.

Experimental results of the raw echo samples and the processed samples, where a person firstly walks towards and then away from the radar, are presented in Fig. 8 (a) and (b), respectively.

Compared with the MABS (Fig. 8 (d)), whose output has tailings, the HLF shows a good performance (Fig. 8 (c)).

TABLE I PARAMETER SETTINGS OF THE EXPERIMENTAL SYSTEM

Parameter	Value
Pulse generator (1st order Gaussian pulse)	
Lower −10dB cutoff frequency	0.45GHz
Upper −10dB cutoff frequency	3.555GHz
Output power	−14dBm
Sampling system	
Fast-time sampling frequency f_{ft}	20GHz
Slow-time sampling frequency f_{st}	20Hz
Total sampling points in fast-time N_{ft}	850
Antenna	
Bandwidth	0.520~5.475GHz

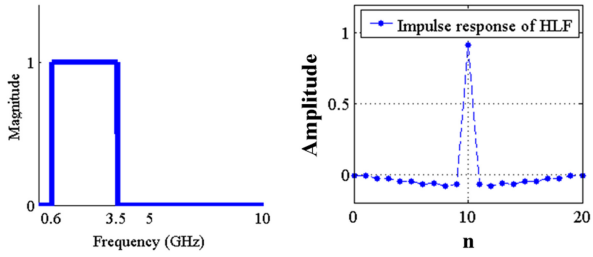

Fig. 7 **(a)** The rectangle window used in the FTFW. **(b)** The impulse response of the FIR HLF, whose magnitude response and phase response have been presented in Fig. 6.

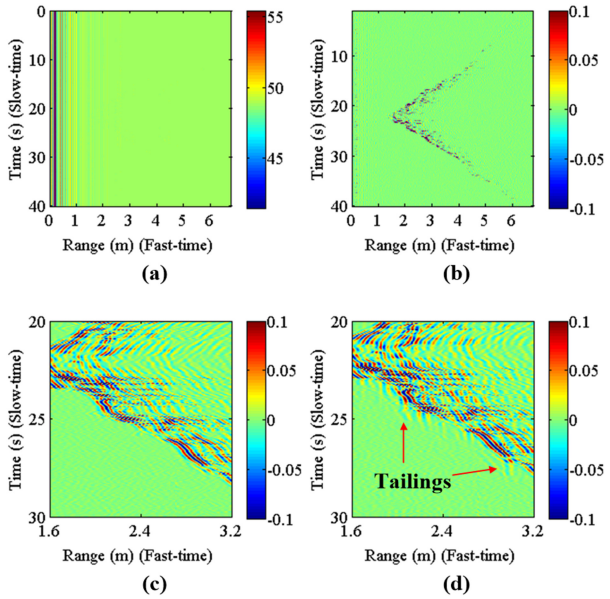

Fig. 8 **(a)** Experimental result of raw echo samples. **(b)** Experimental result of processed samples. **(c)** A zoomed view of the corresponding section from (b). **(d)** Experimental result of processed samples when the MABS is adopted as the slow-time signal processing technique.

IV. Threshold Decision

In previous works [9, 12], the macro-motion was identified by manual inspection from the processed echo samples, where the strong stationary clutter had been removed effectively. There appears to be little relevant work in offering a threshold-decision method, which is useful in applications requiring automatic detection. In this section, a fast-time energy detector [13] is offered to detect the macro-motion. According to Eq. 1 of [13], we need firstly compute the signal energy, and then normalize it by the noise power. In fast-time, the test statistic of the energy detector for the macro-motion signal can be represented as

$$L(n_0) = \frac{\sum_{n=n_0}^{n_0+\Delta n-1}(s[n])^2}{\hat{\sigma}^2}, \quad (6)$$

where $s[n]$ denotes a path of fast-time processed samples, n_0 denotes the initial time of the integration, Δn denotes the time interval of the integration, and $\hat{\sigma}^2$ is a noise power estimate.

In fast-time, the output of the MS algorithm in Fig. 5 mainly contains the echo of the radar impulse and the noise, which is manifested in Fig. 9 (a) from the angle of the fast-time frequency spectrum. Similar to the noise power estimator [1] based on the slow-time FFT proposed in [6] (Eq. 15 and 16 of [6]), a fast-time-FFT-based estimator of the noise power is derived, from the fact that there exists a frequency band in fast-time that only contains the noise, e.g., the frequency band of $f_0 \sim f_1$ shown in Fig. 9 (a), as follows,

$$\hat{\sigma}^2 = \frac{\sum_{k=k_0}^{k_1}|X[k]|^2}{N_{ft}(k_1-k_0+1)}, \quad (7)$$

where $X[k]$ denotes the fast-time FFT of the output of the MS algorithm, $k_0 = \lfloor N_{ft}f_0/f_{ft} \rfloor$, $k_1 = \lfloor N_{ft}f_1/f_{ft} \rfloor$, and $\lfloor x \rfloor$ equals the nearest integer less than or equal to x.

The experimental result of the threshold decision method is presented in Fig. 9 (b). In the near range cells, the crosstalk of the radar system produces many false alarms, which can be prevented by setting a larger threshold in these cells.

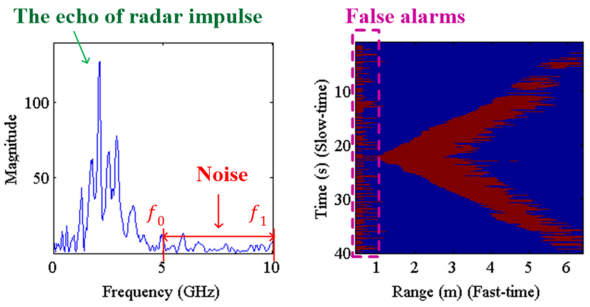

Fig. 9 **(a)** Fast-time frequency spectrum from an experimental output of the MS algorithm in Fig. 5. **(b)** Experimental result of the proposed threshold decision method, where $\Delta n = 100$, $f_0 = 5$GHz, $f_1 = 10$GHz, the threshold is 0.2, and the red region indicates that the macro-motion signal is identified.

[1] The estimator proposed in [6] cannot be used in the macro-motion detection. According to the conclusion of section II, the energy of the motion signal spreads over a quite wide frequency range in slow-time, resulting that we cannot find such a frequency band in slow-time that contains noise only, which is necessary for the noise power estimation method proposed in [6].

V. Conclusion

In this paper, the preprocessing algorithms and the threshold decision method for the macro-motion detection using UWB impulse radar have been studied. First, by a frequency domain analysis, the slow-time motion signal has been shown to be a bandpass signal. Second, in order to avoid the reduction of the measuring range caused by the fast-time filtering, the FTFW has been proposed to process the echo samples in fast-time, and in order to preserve the slow-time motion signal effectively, the HLF has been proposed to process the echo samples in slow-time. Third, a threshold decision method based on the energy detector structure has been presented to locate the human body by detecting the human macro-motion.

References

[1] J. Sachs, M. Aftanas, S. Crabbe, M. Drutarovsky, R. Klukas, D. Kocur, *et al.*, "Detection and Tracking of Moving or Trapped People Hidden by Obstacles using Ultra-Wideband Pseudo-Noise Radar," presented at the 2008 European Radar Conference, 2008.

[2] G. Ossberger, T. Buchegger, E. Schimback, A. Stelzer, and R. Weigel, "Non-invasive Respiratory Movement Detection and Monitoring of Hidden Humans using Ultra Wideband Pulse Radar," presented at the Joint UWBST & IWUWBS 2004, Conference Proceedings, 2004.

[3] I. Y. Immoreev, "Practical Application of Ultra-wideband Radars," in *Ultrawideband and Ultrashort Impulse Signals, Proceedings*, 2006, pp. 44-49.

[4] A. Nezirovic, A. G. Yarovoy, and L. P. Ligthart, "Signal Processing for Improved Detection of Trapped Victims Using UWB Radar," *IEEE Transactions on Geoscience and Remote Sensing,* vol. 48, pp. 2005-2014, Apr 2010.

[5] Y. Y. Xu, S. Dai, S. Y. Wu, J. Chen, and G. Y. Fang, "Vital Sign Detection Method Based on Multiple Higher Order Cumulant for Ultrawideband Radar," *IEEE Transactions on Geoscience and Remote Sensing,* vol. 50, pp. 1254-1265, Apr 2012.

[6] X. Li, D. Qiao, Y. Li, and H. Dai, "A Novel Through-wall Respiration Detection Algorithm Using UWB Radar," presented at the Engineering in Medicine and Biology Society (EMBC), 2013 35th Annual International Conference of the IEEE, Osaka, 2013.

[7] L. B. Liu, Z. J. Liu, and B. E. Barrowes, "Through-Wall Bio-Radiolocation With UWB Impulse Radar: Observation, Simulation and Signal Extraction," *IEEE Journal of Selected Topics in Applied Earth Observations and Remote Sensing,* vol. 4, pp. 791-798, Dec 2011.

[8] M. Baboli, O. Boric-Lubecke, and V. Lubecke, "A New Algorithm for Detection of Heart and Respiration Rate with UWB Signals," presented at the 2012 Annual International Conference of the IEEE Engineering in Medicine and Biology Society (EMBC), 2012.

[9] J. Hu, G. F. Zhu, T. Jin, and Z. M. Zhou, "Adaptive Through-Wall Indication of Human Target with Different Motions," *IEEE Geoscience and Remote Sensing Letters,* vol. 11, pp. 911-915, May 2014.

[10] A. Nezirovic, "Stationary Clutter- and Linear-trend Suppression in Impulse-Radar-based Respiratory Motion Detection," presented at the 2011 IEEE International Conference on Ultra-Wideband (ICUWB), 2011.

[11] M. Piccardi, "Background subtraction techniques: a review," *2004 IEEE International Conference on Systems, Man & Cybernetics, Vols 1-7,* pp. 3099-3104, 2004.

[12] R. Zetik, S. Crabbe, J. Krajnak, P. Peyerl, J. Sachs, and R. Thoma, "Detection and localization of persons behind obstacles using M-sequence through-the-wall radar - art. no. 62010I," *Sensors, and Command, Control, Communications, and Intelligence (C31)Technologies for Homeland Security and Homeland Defense V,* vol. 6201, pp. I2010-I2010, 2006.

[13] H. Urkowitz, "Energy detection of unknown deterministic signals," *Proceedings of the IEEE,* vol. 55, p. 9, 1967.

[14] A. Lazaro, D. Girbau, and R. Villarino, "Analysis of Vital Signs Monitoring Using an Ir-Uwb Radar," *Progress in Electromagnetics Research-Pier,* vol. 100, pp. 265-284, 2010.